

Spontaneous recombination volumes of Frenkel defects in neutron-irradiated non-fcc metals

M. Nakagawa,* W. Mansel, K. Böning, P. Rosner, and G. Vogl†

Physik-Department, Technische Universität München, D-8046 Garching, Germany

(Received 24 April 1978)

Production and production-rate curves for the non-fcc metals Fe, Mo, Ta, W, Zr, and Sn are obtained by electrical-resistivity measurements taken at 4.6 K during reactor neutron irradiations. The saturation concentration of Frenkel defects, c_s , and the recombination volume v_0 are evaluated. A parabolic relation between the spontaneous recombination volume v_0 and the compressibility κ for a series of bcc metals is found.

I. INTRODUCTION

In contrast to fcc metals, much less radiation-damage studies exist on bcc and hcp metals. Furthermore, data on production rate of Frenkel defects and spontaneous recombination volumes are not unique for the non-fcc metals. In a recent study of neutron-irradiated V and Mo,¹ it has been pointed out that the spontaneous recombination volumes of these two bcc metals differed by more than a factor of 3. These facts are contrary to the suggestion made by Horak and Blewitt² according to which bcc metals, in general, have an abnormally low recombination volume compared with fcc metals. In connection with this problem, Biget *et al.*³ suggested a relationship between the spontaneous recombination volumes v_0 of several bcc metals and their compressibilities. However, numerical results on recombination volumes were obtained, in general, from only low-dose experiments. Therefore, the parabolic relationship was, in our opinion, essentially qualitative. In the past, low-temperature fast-neutron irradiation experiments on superconducting materials including Nb, V, and Ta were also performed by Brown *et al.*⁴ However, the scatter of the experimental points in production-rate curves was too large to obtain reliable data on

saturation resistivities and recombination volumes.

In this work we report about damage-rate measurements during fast-neutron irradiation at 4.6 K on the bcc metals Fe, Mo, Ta, and W, the hcp metal Zr, and the tetragonal metal β -Sn. These measurements are related to a similar study on fcc metals.⁵ The irradiation were performed up to integrated doses of 2.39×10^{18} fast neutrons/cm², in two cases (Fe and Sn) to about 10^{19} fast neutrons/cm². The damage rate was monitored by electrical-resistivity measurements.

II. EXPERIMENTAL

All relevant details of the samples are collected in Table I. The polycrystalline sample wires (diameter D and length L) have been purchased from the indicated companies. The residual resistivity ratios (RRR) $\rho_{297\text{K}}/\rho_{4.6\text{K}}$ are given before and after the annealing treatment. Values of $\rho_0 = \rho_{4.6\text{K}}$ have been determined from the final RRR's using tabulated values⁶ of $\rho_{297\text{K}}$. $\Delta\rho_{\text{max}}$ is the maximum induced electrical resistivity and ϕt_{max} is the corresponding fast neutron dose (for $E > 0.1$ MeV). The residual-resistivity values given in the table are without any size-effect corrections.

TABLE I. Sample specifications. The polycrystalline sample wires (diameter D and length L) have been purchased from the indicated companies. MRC is short for Materials Research Corporation. E.S.P.I. is short for Electronic Space Production, Inc. The residual-resistivity ratios (RRR) $\rho_{297\text{K}}/\rho_{4.6\text{K}}$ are given before and after the annealing treatment. Values of $\rho_0 = \rho_{4.6\text{K}}$ have been determined (always without any size-effect correction) from the final RRR's using tabulated values (Ref. 6) of $\rho_{297\text{K}}$. $\Delta\rho_{\text{max}}$ is the maximum induced electrical resistivity and ϕt_{max} is the corresponding fast-neutron dose (for $E > 0.1$ MeV).

No.	Samples Company	$D \times L$ (mm ²)	RRR	Preirradiation annealing			RRR	$\rho_{297\text{K}}$ ($n\Omega$ cm)	ρ_0 ($n\Omega$ cm)	$\Delta\rho_{\text{max}}$ ($n\Omega$ cm)	ϕt_{max} (10^{18} n/cm ²)
				Temperature	Torr	Time					
Fe	Johnson-M.	0.20 × 300	16	800°C,	2×10^{-5} Torr,	2 h	76	10298	135.5	4208.2	8.25
Mo	MRC 99.9%	0.26 × 300	11	2200°C,	2×10^{-5} Torr,	15 m	19	5504	289.7	948.2	2.39
Ta(1)	MRC 99.99%	0.27 × 300	90	2200°C,	5×10^{-10} Torr,	15 m	857	13198	15.39	689.8	2.53
Ta(2)	MRC 99.99%	0.27 × 300	90	2200°C,	4×10^{-10} Torr,	15 m	715	13227	18.45	645.8	2.36
W	Osram	0.18 × 50	40	40	5416	135.4	922.8	2.36
Zr(1)	MRC 99.99%	0.27 × 300	77	77	42966	558.0	4819.2	2.50
Zr(2)	MRC 99.99%	0.27 × 300	77	77	42989	558.3	4625.2	2.39
Sn	E.S.P.I.	0.2 × 300	8090	8090	10994	1.359	491.8	10.25

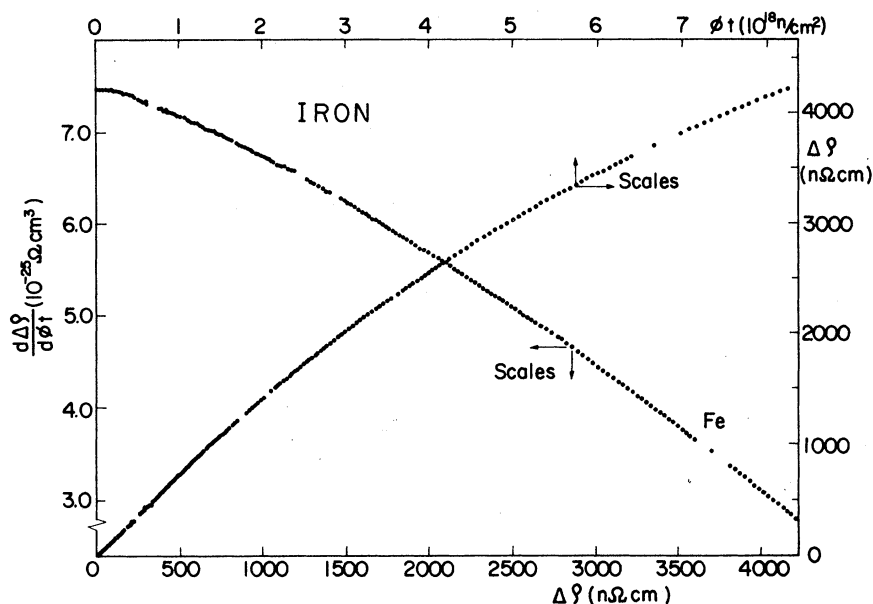


FIG. 1. Increase of residual resistivity $\Delta\rho$ as a function of fast-neutron dose ϕt (right-hand-side and top scales) and differentiated plot $d\Delta\rho/d\phi t$ as a function of $\Delta\rho$ (left-hand-side and bottom scales) for Fe. ϕt is defined for neutron energies $E > 0.1$ MeV. Irradiations and all measurements (*in situ*) have been done at 4.6 K.

Irradiations were performed at 4.6 K in the liquid-helium irradiation facility of the Munich Research Reactor (FRM). The nominal value of the local fast-neutron flux ϕ_0 ($E > 0.1$ MeV) was 1.3×10^{13} n/cm² sec; the corresponding resonance flux (related to the gold resonance) was 1.2×10^{12} n/cm² sec and the thermal flux was 1.5×10^{13} n/cm² sec. Details about the flux spectrum, the sample holder, and the resistivity measurement apparatus are given in Ref. 5. In order to record the evolution of the defect production with increasing neutron doses, we have irradiated Fe during 183 h 45 min (i.e., up to integrated doses of 8.25×10^{18} fast neutrons/cm²), Sn during 213 h 30 min

(10.25×10^{18} fast neutrons/cm²), and Mo, Ta, W, and Zr during 52 h 40 min [$(2.36-2.53) \times 10^{18}$ fast-neutrons/cm²]. More than 200 resistivity measurements were performed during the irradiations of Fe and Sn, and more than 80 measurements for Mo, Ta, W, and Zr.

III. RESULTS AND DISCUSSION

The experimental results for the increase $\Delta\rho$ of residual resistivity with irradiation dose ϕt are given in the Figs. 1-6. The derived resistivity damage rates $d\Delta\rho/d\phi t$ as a function of $\Delta\rho$ are also given in these figures.

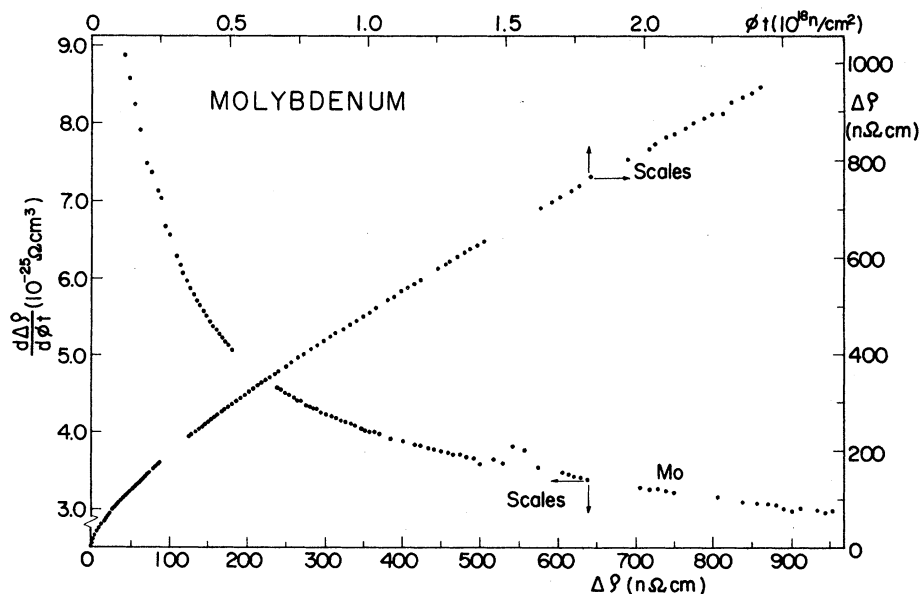


FIG. 2. Dose-curve results for Mo. For the presentation of the data see caption of Fig. 1.

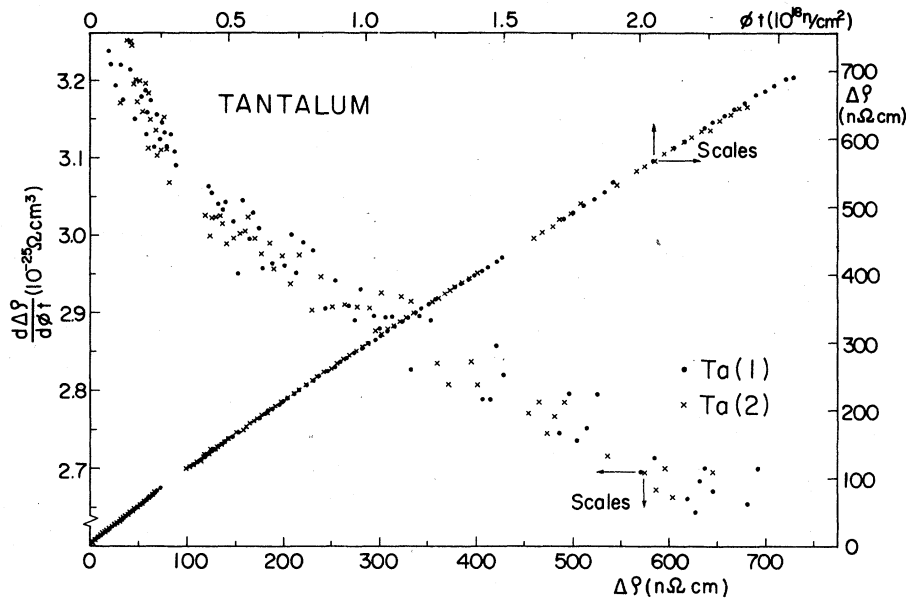


FIG. 3. Dose-curve results for Ta. Both two series of plots of $\Delta\rho$ vs ϕt and two differentiated plots are shown. For the presentation of the data see caption of Fig. 1.

As was shown in Ref. 5, the production-rate curves can be analyzed in terms of a third-order polynomial,

$$\frac{d\Delta\rho}{d\phi t} = A + B\Delta\rho + C\Delta\rho^2 + D\Delta\rho^3, \quad (1)$$

or a second-order polynomial,

$$\frac{d\Delta\rho}{d\phi t} = A + B\Delta\rho + C\Delta\rho^2. \quad (2)$$

According to the theory of Lück and Sizmann⁷ also

a linear relation between $d\Delta\rho/d\phi t$ and $\Delta\rho$ is obtained,

$$\frac{d\Delta\rho}{d\phi t} = A \left(1 - 2v_0 \frac{\Delta\rho}{\rho_F} \right), \quad (3)$$

where ρ_F is the Frenkel-defect specific resistivity and v_0 is the spontaneous recombination volume.

For Fe and Sn both quadratic and linear fits were applied (for cubic fits, see Ref. 5). In the case of other samples, in addition to the relatively small neutron doses and great "tail" in the beginning of the irradiation, the scatter of the experi-

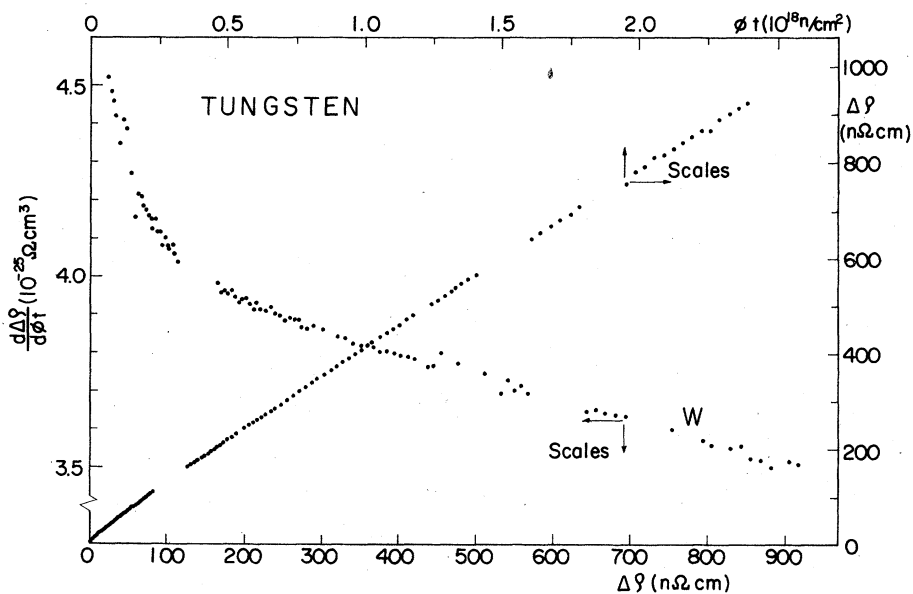


FIG. 4. Dose-curve results for W. For the presentation of the data see caption of Fig. 1.

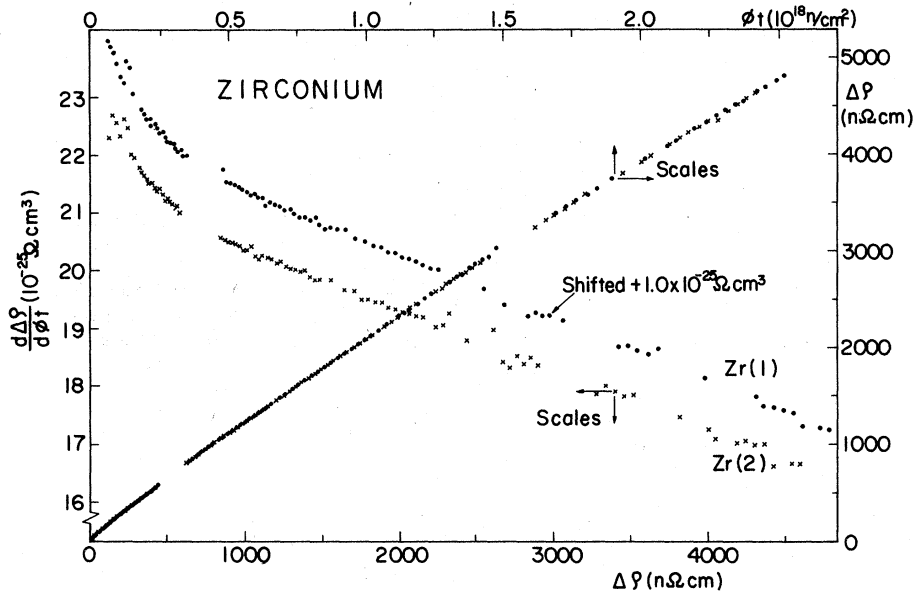


FIG. 5. Dose-curve results for Zr. Two series of plots of $\Delta\rho$ versus ϕt are shown (right-hand-side and top scales) and the differentiated plots $d\Delta\rho/d\phi t$ vs $\Delta\rho$ are shown for two samples. For Zr(1), the ordinate is shifted up by $1.0 \times 10^{-25} \Omega \text{ cm}^3$. For the other presentation of the data, see captions of Fig. 1.

mental points was too large to permit a preference as to the linear or quadratic fit; thus, we have made only a linear evaluation for these metals. The linear fit was done for all but the first "tail" points.

The extrapolation of the damage rate curves towards zero-change rate leads to the saturation resistivity $\Delta\rho_s$ which is given in Table II. In this case one obtains from Eq. (3) for the spontaneous recombination volume the expression

$$v_0 = \rho_F / 2\Delta\rho_s \quad (4)$$

Using Eq. (2) one obtains for the spontaneous re-

combination volume according to Refs. 5 and 8

$$v_0 = \rho_F / \Delta\rho_s \quad (5)$$

Thus calculated values of the spontaneous recombination volumes are given in Table II together with values taken from the literature.

By the way, the characteristic resistivity of a Frenkel pair, ρ_F , is a fundamental parameter in these studies, so the significance of its choice has been discussed in great detail in Refs. 1 and 9. However, we prefer to choose ρ_F values same as in Ref. 3 to simplify the comparison with results in the past.

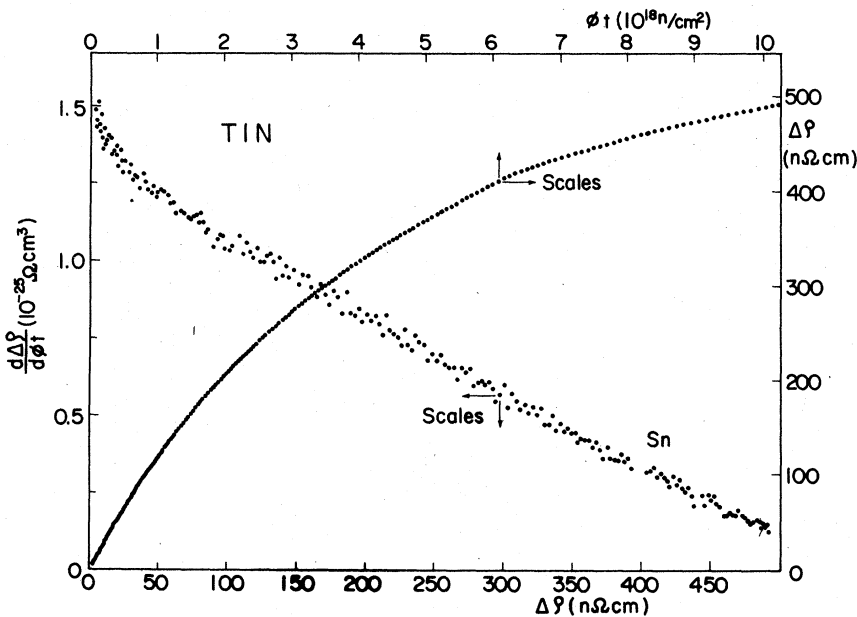


FIG. 6. Dose-curve results for Sn. For the presentation of the data see caption of Fig. 1.

TABLE II. Results of the quadratic (for Fe and Sn) and linear fits to the production rate curves. The values ρ_F (defined by $\Delta\rho = c\rho_F$) are taken from the literature. $\Delta\rho_s$ is the extrapolated saturation resistivity and v_0 is the recombination volume as calculated from Eq. (4) or (5). The compressibility κ is taken from Ref. 24.

Samples	$\Delta\rho_{\max}$	$\Delta\rho_s$ (fit) ($n\Omega$ cm)	ρ_F ($\mu\Omega$ cm/at. %)		$c_s = \Delta\rho_s/\rho_F$ (10^{-3} at. fraction)	Ours v_0 (at. vol.)	Literature v_0 (at. vol.)	κ (10^{-12} cm ² /dyn)	
Fe	4208.2	6300 \pm 200 (lin.)	19	Ref. 2	3.32 \pm 0.10	151 \pm 5	105	0.589	
		5800 \pm 100 (quadr.)				3.05 \pm 0.05	328 \pm 6		43 ~ 67
Mo	948.2	5260 \pm 760 (lin.)	13 \pm 2	Ref. 9	4.05 \pm 0.58	124 \pm 18	200 \pm 30 120 ~ 155	Ref. 3 Ref. 2	0.383
Ta(1)	689.8	4450 \pm 200 (lin.)	17.5	Ref. 18	2.54 \pm 0.11	197 \pm 9	240 \pm 40	Ref. 3	0.510
Ta(2)	645.8						280	Ref. 20	
W	922.8	7140 \pm 680 (lin.)	13	Ref. 3	5.49 \pm 0.52	91 \pm 9	190	Ref. 3	0.321
Zr(1)	4819.2	20000 \pm 500 (lin.)	40	Ref. 22	5.00 \pm 0.13	100 \pm 3	195 \pm 17	Ref. 21	...
Zr(2)	4625.2	20500 \pm 500 (lin.)				5.10 \pm 0.13			
Sn	491.8	536 \pm 10 (lin.)	1.1	Ref. 23	4.87 \pm 0.09	103 \pm 2
		558 \pm 10 (quadr.)				5.07 \pm 0.09			

A. Iron (Fig. 1)

The striking feature of the production rate curve of Fe is the negative (convex) curvature.¹⁰ This behavior, indeed, represents a realistic physical effect and not, for example, an experimental artifact. The sample temperature was always that of liquid helium. Any possible (although probably negligible) change of the local neutron spectrum during a period of continuous reactor operation should be much more pronounced during the first 30 h of operation (buildup of the ¹³⁵Xe poisoning) than in the remaining 170 h. Note that the defect production curves of other metals as Al, which according to Ref. 5 were contained in the same sample holder as the Fe sample of this paper, are perfectly regular and exhibit the usual positive (concave) curvature without any particularity around $\phi t = 1.4 \times 10^{18}$ n/cm² (corresponding to 30 h as mentioned above); this also demonstrates that our continuous local-fast-neutron-flux monitor, which uses the ¹⁶O(n, p)¹⁶N reaction and so measures only the fastest neutrons having energies above 10 MeV, indeed provides a realistic information about the "fast-flux" ϕ and that changes of the neutron spectrum within a reactor operation period are insignificant.

Previously, Horak and Blewitt² obtained results for the differentiated dose curve of reactor-irradiated Fe which are also consistent with a negative curvature, although the larger scatter of the data and the much smaller irradiation dose did not allow them to clearly recognize this effect. More recently the convex curvature has been confirmed

in independent low-temperature reactor irradiations of Fe in Garching-Munich¹¹ and Paris.¹² The magnitude and dose range of the convex curvature seems to depend on the purity of the Fe samples and on the type of irradiating particles since the effect obviously does not occur during electron¹² or fission-fragment¹³ irradiation. The negative curvature of the differentiated dose curve of Fe, which has also been observed during reactor irradiation of Ni, Pd, and Pt,⁵ cannot be explained within the framework of usual defect production theory since the overlap of recombination volumes v_0 would always lead to a positive (concave) curvature.¹⁴ Very probably the negative curvature is caused by a decrease of the electrical resistivity per Frenkel defect, when the individual displacement cascades overlap during high-dose reactor irradiation leading to the growth and to configuration changes of the defect clusters.^{5,11}

The results of a computer fit for Eq. (2) was best with $B/A = -9.91 \times 10^{-5}$ (n Ω cm)⁻¹ and $C/A = -1.25 \times 10^{-8}$ (n Ω cm)⁻², and for $\Delta\rho > 70$ n Ω cm the fit deviation was always smaller than 0.04×10^{-25} Ω cm³. From this high-dose fit we obtained the saturation resistivity $\Delta\rho_s = 5800$ n Ω cm, a value which is significantly smaller than the low-dose extrapolation result ($\Delta\rho_s = 9230$ n Ω cm) of Horak and Blewitt.² Assuming $\rho_F = 19$ $\mu\Omega$ cm/at.%,¹⁵ we obtain from Eq. (5) $v_0 \approx 330$ at. vol.

Horak and Blewitt used the value $\rho_F = 12.5$ $\mu\Omega$ cm/at. % and obtained $v_0 = 43-67$ at. vol. (i.e., 65-101 at. vol., if $\rho_F = 19$ $\mu\Omega$ cm/at. % is applied). Biget *et al.* adopted the value $v_0 = 105$ at. vol. In any case, our result $v_0 \approx 330$ at. vol. for the spontan-

eous recombination volume of Fe is larger by a factor 3 to 5 than the other.

For reference, the results of the computer fit for Eq. (3) (linear fit) are also listed on the upper row in third, fifth, and sixth columns in Table II. In case of the linear fit, we obtain from Eq. (4) $v_0 \approx 150$ at. vol.

On the other hand, an irradiation experiment at 20 K by fission fragments¹⁶ shows $\Delta\rho_s = 3000\text{--}4000$ n Ω cm (quadratic fit) for Fe and suggests much larger recombination volume, though as discussed in Ref. 5 radiation damage by fission fragments might be different from that by neutrons.

B. Molybdenum (Fig. 2)

There are some experimental data to be compared with our results. Maury *et al.*⁹ determined the Frenkel pair resistivity from the results of their experiments; $\rho_F = 13 \pm 2$ $\mu\Omega$ cm/at.%. Applying the value determined thus, they get $v_0 = 200\text{--}250$ at. vol. Recently, Biget *et al.* modified this value and adopted $v_0 = 200 \pm 30$ at. vol. in Ref. 3, as listed in Table II. On the other hand, Horak and Blewitt² obtained $v_0 = 120\text{--}155$ at. vol., assuming $\rho_F = 10$ $\mu\Omega$ cm/at. %.

As seen in Fig. 2, Mo shows a great "tail" which is interpreted as stemming from long-range collision sequences.¹⁷ From the rest of the points, we have calculated the saturation resistivity by a linear fit, leading to the recombination volume $v_0 = 124$ at. vol. This value is smaller by factor of $\frac{2}{3}$ than that of Biget *et al.*³

C. Tantalum (Fig. 3)

Biget *et al.*³ have taken $\rho_F = 17.5$ $\mu\Omega$ cm/at. % as determined by Jung and Schilling¹⁸ and obtained $v_0 = 240 \pm 40$ at. vol. using the saturation resistivity of Ta irradiated by electrons.¹⁹ Biget *et al.* have also listed $\rho_F = 24$ $\mu\Omega$ cm/at. % $\approx 2\rho_0$ in their table. However, in our opinion, the relation $\rho_F \approx 2\rho_0$ is only a criterion for unestablished values of elements. On the other hand, Faber²⁰ has obtained $v_0 = 280$ at. vol., assuming $\rho_F = 17$ $\mu\Omega$ cm/at. %. Our result $v_0 = 197$ at. vol. for Ta is smaller by factor of $\frac{2}{3}$ than that of Ref. 20.

D. Tungsten (Fig. 4)

Biget *et al.* have taken $\rho_F = 13$ $\mu\Omega$ cm/at. % of Frenkel pairs, in view of the close resemblance in the electrical properties of Mo and W and presented the value $v_0 = 190$ at. vol.³ Our result $v_0 = 91$ at. vol. for W is much smaller by a factor of $\frac{1}{2}$ than that of the above-mentioned low-dose data.

The fission-fragments irradiation experiment¹⁶ gave the saturation resistivity $\Delta\rho_s \sim 8000$ n Ω cm. Assuming $\rho_F = 13$ $\mu\Omega$ cm/at. % one obtains $v_0 = 80$

at. vol., which closely resembles our result.

E. Zirconium (Fig. 5)

Vialaret *et al.*²¹ performed electrical-resistivity measurements to study the creation and annealing out of defects in Zr irradiated at 24 K by fast neutrons. They obtained an apparent recombination volume of 195 ± 17 at. vol. independent of oxygen content using the resistivity per Frenkel pair $\rho_F = 40$ $\mu\Omega$ cm/at. % after Biget *et al.*²² The maximum induced resistivity was about 2500 n Ω cm, which was only a half of ours.

Although a large scatter of the experimental points exists in our measurement, we obtain $v_0 = 98 \sim 100$ at. vol. from the linear fit as listed in Table II. The discrepancy between ours and Vialaret *et al.*'s values of a factor of 2 may come from the difference of the irradiation temperature. Further experiments on Zr and on other hcp metals, such as Mg, Ti, Co, and Zn, are very desirable.

F. Tin (β -Sn) (Fig. 6)

Tin has no other data to be compared with our results. In this experiment, the fluctuation of the data was not small, so we could not choose decidedly between quadratic and cubic fits. Saturation values from above fits are 558 and 544 n Ω cm for quadratic and cubic fits, respectively. Assuming the resistivity of Frenkel pair $\rho_F = 1.1$ $\mu\Omega$ cm/at. %, ²³ we obtain $v_0 = 200$ at. vol. In the cases of the linear fit, for reference, we obtain from Eq. (4) $v_0 = 103$ at. vol. as listed in Table II.

G. Parabolic relation between the spontaneous recombination volume and the compressibility

It was suggested by Biget *et al.*³ that there is a relationship between the spontaneous recombination volumes and the compressibility of the bcc metals. For W, Mo, Ta, Nb, and V they found a power law of roughly second order. In Fig. 7 we have now plotted our values of the spontaneous

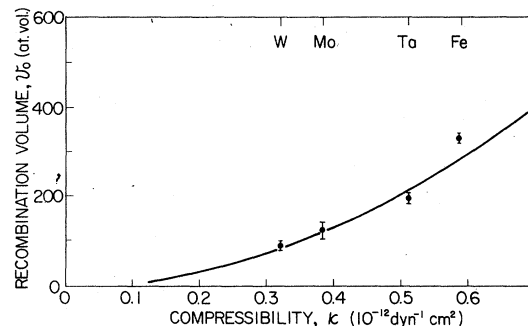


FIG. 7. Spontaneous recombination volume v_0 of several bcc metals as a function of their compressibility κ .

recombination volumes v_0 as a function of the compressibility κ . The values of κ are taken from Ref. 24 (see Table II). We can also put one curve through our points which is roughly of second order, though our values for the recombination volume differ from those of Biget *et al.*³ However, such an analysis has to be taken with caution keeping in mind the uncertainty of the spontaneous recombination volumes due to the uncertainty of the values of ρ_F .

IV. SUMMARY

Polycrystalline wires have been irradiated at 4.6 K by reactor neutrons ($E > 0.1$ MeV) to a dose of $(2.3-2.5) \times 10^{18}$ n/cm² for Mo, Ta, W, and Zr, 8.25×10^{18} n/cm² for Fe, and 10.25×10^{18} n/cm² for Sn. Production and production rate curves were obtained by electrical-resistivity measurements taken at 4.6 K. Saturation concentration of Frenkel defects c_s and spontaneous recombina-

tion volumes v_0 were evaluated. For Mo, Ta, W, and Zr, v_0 values are by a factor of $\frac{1}{2}$ to $\frac{2}{3}$ smaller, whereas for Fe v_0 is a factor 3 to 5 larger than the values given in the literature for low-dose experiments. A parabolic relation between the spontaneous recombination volume v_0 and the compressibility κ for Fe, Mo, Ta, and W is found.

ACKNOWLEDGMENTS

This research was supported by the German "Bundesministerium für Forschung und Technologie". We are grateful to Professor H. Vonach and Professor W. Gläser for the support of this work and to the staffs of the liquid-helium irradiation facility and of the Research Reactor Munich for their continuous help and cooperations. One of the authors (M.N.) gratefully acknowledges Professor T. Shibata, Director of Research Reactor Institute, Kyoto University, for the opportunity to carry out this research at FRM.

*Present address: Research Reactor Institute, Kyoto University, Kumatori-cho, Osaka 590-04, Japan.

†Present address: Hahn-Meitner-Institut für Kernforschung Berlin GmbH, D-1000 Berlin 39, Germany.

¹P. Vajda and M. Biget, *Phys. Status Solidi A* **23**, 251 (1974).

²J. A. Horak and T. H. Blewitt, *Phys. Status Solidi A* **9**, 721 (1972).

³M. Biget, R. Rizk, P. Vajda, and A. Bessis, *Solid State Commun.* **16**, 949 (1975).

⁴B. S. Brown, T. H. Blewitt, T. L. Scott, and A. C. Klank, *J. Nucl. Mater.* **52**, 215 (1974).

⁵M. Nakagawa, K. Böning, P. Rosner, and G. Vogl, *Phys. Rev. B* **16** 5285 (1977).

⁶*American Institute of Physics Handbook*, 3rd ed. (McGraw-Hill, New York, 1972), Chaps. 9-39.

⁷G. Lück and R. Sizmann, *Phys. Status Solidi* **5**, 683 (1964).

⁸K. Dettmann, G. Leibfried and K. Schroeder, *Phys. Status Solidi* **22**, 423 and 433 (1967).

⁹F. Maury, P. Vajda, M. Biget, A. Lucasson, and P. Lucasson, *Radiat. Eff.* **25**, 175 (1975).

¹⁰M. Nakagawa, K. Böning, P. Rosner, and G. Vogl, *Phys. Lett. A* **56**, 481 (1976).

¹¹B. M. Pande, A. Dunlop, K. Böning, H. E. Schaefer, P. Rosner, and J. C. Jousset (unpublished).

¹²A. Dunlop, J. C. Jousset, and N. Lorenzelly (private communication).

¹³R. C. Birtcher and T. H. Blewitt, *J. Nucl. Mater.* **69&70**, 783 (1978).

¹⁴For example, H. J. Wollenberger, in *Vacancies and Interstitials in Metals* (North-Holland, Amsterdam, 1970), pp. 215-253.

¹⁵A. Lucasson, P. Lucasson, and R. M. Walker, *Proceedings of the International Conference on Properties of Reactor Materials, Berkeley, England*, (Butterworths, London 1961), p. 83.

¹⁶J. Ponsoye, *Radiat. Eff.* **8**, 13 (1971).

¹⁷G. Burger, H. Meissner, and W. Schilling, *Phys. Status Solidi* **4**, 281 (1964).

¹⁸P. Jung and W. Schilling, *Phys. Rev. B* **5**, 2046 (1972).

¹⁹D. Meissner and W. Schilling, *Z. Naturforsch., Teil A* **26**, 502 (1971).

²⁰K. Faber, thesis (University of Stuttgart, 1974).

²¹P. Vialaret, F. Moreau, A. Bessis, C. Dimitrov, and O. Dimitrov, *J. Nucl. Mater.* **55**, 83 (1975).

²²M. Biget, F. Maury, P. Vajda, A. Lucasson, and P. Lucasson, *Radiat. Eff.* **7**, 223 (1971).

²³J. McIlwain, R. Gardiner, A. Sosin, and S. Myhra, *Radiat. Eff.* **24**, 19 (1975).

²⁴Smithells, *Metals Reference Book*, 4th ed. (Butterworths, London, 1967), Vol. 3, p. 708.